

Accelerated growth of B16BL6 tumor in mice through efficient uptake of their own exosomes by B16BL6 cells

Akihiro Matsumoto,¹  Yuki Takahashi,¹ Makiya Nishikawa,¹ Kohei Sano,² Masaki Morishita,¹ Chonlada Charoenviriyakul,¹ Hideo Saji² and Yoshinobu Takakura¹

Departments of ¹Biopharmaceutics and Drug Metabolism; ²Patho-Functional Bioanalysis, Graduate School of Pharmaceutical Sciences, Kyoto University, Sakyo-ku, Kyoto, Japan

Key words

Biodistribution, exosomes, melanoma, proliferation, uptake

Correspondence

Yuki Takahashi, Department of Biopharmaceutics and Drug Metabolism, Graduate School of Pharmaceutical Sciences, Kyoto University, Sakyo-ku, Kyoto 606-8501, Japan.

Tel: +81-75-753-4616; Fax: +81-75-753-4614;
E-mail: ytakahashi@pharm.kyoto-u.ac.jp

Funding Information

This work was supported by Takeda Science Foundation.

Received May 3, 2017; Revised June 20, 2017; Accepted June 28, 2017

Cancer Sci 108 (2017) 1803–1810

doi: 10.1111/cas.13310

Exosomes are extracellular vesicles released by various cell types and play roles in cell–cell communication. Several studies indicate that cancer cell-derived exosomes play important pathophysiological roles in tumor progression. Biodistribution of cancer cell-derived exosomes in tumor tissue is an important factor for determining their role in tumor proliferation; however, limited studies have assessed the biodistribution of exosomes in tumor tissues. In the present study, we examined the effect of cancer-cell derived exosomes on tumor growth by analyzing their biodistribution. Murine melanoma B16BL6-derived exosomes increased the proliferation and inhibited the apoptosis of B16BL6 cells, which was associated with an increase and decrease in the levels of proliferation- and apoptosis-related proteins, respectively. GW4869-induced inhibition of exosome secretion decreased the proliferation of B16BL6 cells, and treatment of GW4869-treated cells with B16BL6-derived exosomes restored their proliferation. Next, we treated B16BL6 tumors in mice with B16BL6-derived exosomes and examined the biodistribution and cellular uptake of these exosomes. After the intratumoral injection of radiolabeled B16BL6-derived exosomes, most radioactivity was detected within the tumor tissues of mice. Fractionation of cells present in the tumor tissue showed that fluorescently labeled exosomes were mainly taken up by B16BL6 cells. Moreover, intratumoral injection of B16BL6-derived exosomes promoted tumor growth, whereas intratumoral injection of GW4869 suppressed tumor growth. These results indicate that B16BL6 cells secrete and take up their own exosomes to induce their proliferation and inhibit their apoptosis, which promotes tumor progression.

Exosomes are extracellular vesicles released by various cell types.⁽¹⁾ Exosomes package proteins and nucleic acids and function as endogenous delivery carriers in cell–cell communication.⁽¹⁾ Because cancer cells also secrete exosomes, several studies have investigated the role of cancer cell-derived exosomes in cancer biology.⁽²⁾ Detection of primary tumor tissue-secreted exosomes in specific organs and determination of their role in the initiation of pre-metastatic niche formation has led to detailed research on molecular mechanisms underlying the role of these exosomes in cancer metastasis.^(3–5) Recent studies indicate that specific proteins and microRNAs present in cancer cell-derived exosomes determined organotropic metastasis.^(6,7)

In vitro studies assessing the biological roles of cancer cell-derived exosomes have shown that these exosomes promote tumor progression by affecting different cell types.^(8,9) To determine the actual effect of cancer cell-derived exosomes, it is important to analyze their *in vivo* behavior. However, limited information is available on the transport of cancer cell-derived exosomes from tumor tissue to other organs and on cell types involved in their uptake.

Exosome labeling technology that allows high sensitive and quantitative analysis would be useful for understanding the *in vivo* behavior of exosomes.^(10,11) Previously, we developed an exosome radiolabeling method based on streptavidin (SAV)-biotin interaction by designing a fusion protein containing SAV and lactadherin (LA; an exosome-tropic protein) called SAV-LA.⁽¹⁰⁾ Exosomes were radiolabeled by incubating SAV-LA-modified exosomes with an iodine-125 (¹²⁵I)-labeled biotin derivative. The radiolabeled exosomes were then intravenously injected into mice, and their pharmacokinetic characteristics were evaluated.⁽¹⁰⁾ In addition, we previously used fluorescently labeled exosomes to determine cell types involved in exosome uptake in the liver, spleen, and lungs.⁽¹²⁾ Based on the results of these studies, we aimed to determine the *in vivo* behavior of cancer cell-derived exosomes administered exogenously.

In the present study, we selected murine melanoma B16BL6 cells as model cancer cells and determined the effects of B16BL6-derived exosomes on these cells. In addition, we directly injected B16BL6-derived exosomes into B16BL6 tumors in mice and examined their biodistribution, cellular

uptake, and effect on tumor growth. Finally, we investigated the effects of GW4869, an inhibitor of exosome secretion, on tumor growth. Our results clearly showed that B16BL6-derived exosomes were efficiently taken up by B16BL6 tumor cells and accelerated the growth of these cells.

Materials and Methods

Mice. Five-week-old male C57BL/6J mice were purchased from Japan SLC, Inc. (Shizuoka, Japan). Protocols for all animal experiments were approved by the Animal Experimentation Committee of the Graduate School of Pharmaceutical Sciences of Kyoto University.

Cell culture. B16BL6 murine melanoma cells were obtained from Riken BioResource Center (Tsukuba, Japan) and were cultured in Dulbecco's modified Eagle's medium (DMEM) supplemented with 10% heat-inactivated fetal bovine serum (FBS), 0.15% sodium bicarbonate, 100 IU/mL penicillin, 100 µg/mL streptomycin, and 2 mM L-glutamine at 37°C in a humidified atmosphere containing 5% CO₂.

Exosome collection. Exosomes were collected from the culture supernatant of B16BL6 cells by performing differential centrifugation followed by ultracentrifugation, as described previously.⁽¹³⁾ In brief, cell supernatants were centrifuged at 300 g for 10 min, 2000 g for 20 min, and 10 000 g for 30 min in order to remove cell debris and microvesicles including apoptotic bodies. The supernatant was passed through 0.22 µm syringe filter, followed by 100 000 g for 1 h using a Hitachi CP80WX ultracentrifuge (Hitachi High-Technologies, Tokyo, Japan). The exosome pellet was washed in phosphate buffered saline (PBS), centrifuged at 100 000 g for 1 h and resuspended in PBS. The amount of exosomes collected was estimated by measuring protein concentration by performing Bradford assay. Presence of exosome marker proteins Alix, HSP70, and CD81 and absence of negative marker protein calnexin in the collected exosomes was confirmed by performing western blotting with the same antibodies and protocol as those described previously.⁽¹³⁾

Electron microscopic observation and measurement of particle size of exosomes. The exosome suspension was added to an equal volume of 4% paraformaldehyde (Nacalai Tesque, Kyoto, Japan), and the mixture was applied to a Formvar/Carbon film-coated transmission electron microscope (TEM) grid (Alliance Biosystems, Osaka, Japan). The sample was then washed with PBS. Then, the sample was fixed by incubation with 1% glutaraldehyde for 5 min, washed with PBS, and incubated with 1% uranyl acetate for 5 min. The sample was observed under a TEM (Hitachi H-7650; Hitachi High-Technologies). A qNano instrument (Izon Science Ltd., Christchurch, New Zealand) was used to measure the particle size distribution of the exosomes.

Preparation of fluorescently labeled exosomes. PKH26 red fluorescent cell linker kit and PKH67 green fluorescent cell linker kit were obtained from Sigma-Aldrich (St. Louis, MO, USA). Exosomes were labeled with PKH dyes (PKH26 and PKH67), as described previously.⁽¹²⁾ Briefly, exosomes resuspended in a buffer provided in the kits were mixed with the PKH dyes and were incubated for 5 min at room temperature. Next, the samples were added to phosphate-buffered saline (PBS) supplemented with 5% bovine serum albumin and were ultracentrifuged at 100 000 g for 1 h to remove free dyes.

Uptake of exosomes by B16BL6 cells. For this, 1×10^5 B16BL6 cells were seeded onto a chamber slide (WATSON CO., LTD, Kobe, Japan) 1 day before the experiment. Next,

10 µg/mL PKH26-labeled exosomes were added to the cell culture, and the cells were incubated for 4 or 24 h. The cells were washed twice with PBS, fixed with 4% paraformaldehyde for 20 min, and washed twice again with PBS. Next, the cells were treated with 100 nM 4',6-diamino-2-phenylindole (DAPI) for 5 min to stain their nuclei and were washed once with PBS. Finally, the cells on the slide were examined using a confocal laser-scanning microscope (A1R-MP; Nikon Instech Co., Ltd., Tokyo, Japan).

In a separate experiment, 1×10^5 B16BL6 cells were seeded in a 24-well plate. After 24 h of incubation, indicated concentrations of PKH67-labeled exosomes were added to the cell culture and the cells were incubated for 4 or 24 h. Next, the cells were washed twice with PBS and were harvested. Mean fluorescence intensity (MFI) of the cells was determined using a flow cytometer (Gallios Flow Cytometer; Beckman Coulter, Miami, FL, USA). Data were analyzed using Kaluza software (version 1.0; Beckman Coulter).

Tumor cell proliferation assay. For this, 5×10^3 B16BL6 cells were seeded in a 96-well plate containing DMEM lacking FBS 1 day before the experiment. The cells were then incubated with the indicated concentrations of B16BL6-derived exosomes or 10% normal FBS for 24 h, and cell numbers were determined using MTT assay kit (Nacalai Tesque).

Flow cytometric determination of apoptotic cells. For this, 1×10^5 B16BL6 cells were seeded in a 24-well plate containing DMEM supplemented with the indicated concentrations of B16BL6-derived exosomes and without FBS. After 24 h, cells both on the plate and in the medium were harvested. Apoptotic cells were determined using Alexa Fluor 488 annexin V (AnV)/propidium iodide (PI) apoptosis detection kit (Thermo Fisher Scientific, Waltham, MA, USA) and Gallios Flow Cytometer, according to the manufacturer's instructions. Data were analyzed using the Kaluza software.

Western blotting. For this, 2×10^5 B16BL6 cells were seeded in a 12-well plate with or without the indicated concentrations of B16BL6-derived exosomes. After 24 h, the cells were washed twice with PBS and were harvested. Cell lysates were prepared by freezing and thawing the cells five times, followed by centrifugation to remove cell debris. Reduced cell lysates (2 µg) were resolved by performing sodium dodecyl sulfate-polyacrylamide gel electrophoresis on a 10% gel and were transferred onto a polyvinylidene fluoride membrane. Cyclin D1, Bcl-2, Bax, Akt, phosphorylated Akt (p-Akt), and GAPDH were detected by incubating the membrane with the following antibodies for 1 h at room temperature: rabbit anti-cyclin D1 antibody (dilution, 1:1000; Abcam, Cambridge, UK), rabbit anti-Bcl-2 antibody (dilution, 1:1000; Abcam), rabbit anti-Bax antibody (dilution, 1:1000; Abcam), rabbit anti-Akt antibody (dilution, 1:1000; Enzo Biochem, New York, NY, USA), rabbit anti-p-Akt antibody (dilution, 1:200; Santa Cruz Biotechnology, Dallas, TX, USA), and rabbit anti-GAPDH antibody (dilution, 1:10 000; Abcam). Next, the membrane was incubated with goat anti-rabbit IgG-HRP (dilution, 1:5000; Santa Cruz Biotechnology) for 1 h at room temperature. The membrane was then reacted with Immobilon Western Chemiluminescent HRP substrate (Merck Millipore, Billerica, MA, USA), and chemiluminescence was detected using LAS-3000 instrument (FUJIFILM, Tokyo, Japan).

In a separate experiment, proteins present in the exosomes and cell lysates were resolved by performing sodium dodecyl sulfate-polyacrylamide gel electrophoresis and were transferred onto a polyvinylidene fluoride membrane, as described above. Survivin expression was detected by incubating the membrane

with rabbit anti-survivin antibody (dilution, 1:1000; Abcam) for 1 h at room temperature, followed by incubation with goat anti-rabbit IgG-HRP (dilution, 1:5000; Santa Cruz Biotechnology) for 1 h at room temperature. The membrane was then reacted with Immobilon Western Chemiluminescent HRP substrate, and chemiluminescence was detected using the LAS-3000 instrument.

Inhibition of exosome secretion. For this, 8×10^6 B16BL6 cells were seeded in a 15-cm dish and were incubated for 24 h. Next, the cells were incubated with or without 5 $\mu\text{g}/\text{mL}$ GW4869 (dissolved in 5% DMSO; Cayman Chemical, Michigan, MI, USA), an inhibitor of neutral sphingomyelinases, for 24 h at 37°C. Exosomes were collected, and the amount of the collected exosomes was determined by measuring protein concentration. Levels of Alix, HSP70, CD81, and calnexin in the collected samples were determined by performing western blotting, as described previously.

Effect of GW4869 on tumor cell proliferation. For this, 1×10^4 B16BL6 cells were seeded in a 96-well plate 1 day before the experiment. The cells were then incubated with or without 5% DMSO (vehicle), 5 $\mu\text{g}/\text{mL}$ GW4869 and the indicated concentrations of B16BL6-derived exosomes for 24 h, and cell numbers were estimated using the MTT assay kit.

Xenograft tumor model. Mice were subcutaneously inoculated with 5×10^5 B16BL6 cells. Tumor size was measured using a slide caliper, and tumor volume was calculated using the following formula: tumor volume (mm^3) = (longer length \times shorter length²) \times 0.5. All animal experiments were conducted when tumor volume was $>100 \text{ mm}^3$, unless otherwise indicated. Tumor-bearing mice were euthanized once tumor volume reached 3000 mm^3 .

Preparation of ¹²⁵I-labeled B16BL6-derived exosomes. SAV-LA-expressing plasmid (pCMV-SAV-LA) and SAV-LA-modified exosomes were prepared, as described previously.⁽¹⁰⁾ In brief, B16BL6 cells seeded in culture dishes were transfected with pCMV-SAV-LA by using polyethylenimine Max (Polysciences, Warrington, PA, USA). After 24 h, SAV-LA-modified exosomes present in the culture supernatant were collected. The amount of collected exosomes was estimated by measuring protein concentration by performing the Bradford assay. Radiolabeled exosomes were prepared by incubating the SAV-LA-modified exosomes with (3-¹²⁵I-iodobenzoyl) norbiotinamide, an ¹²⁵I-labeled biotin derivative.

Evaluation of the biodistribution of intratumorally injected radiolabeled exosomes in mice. ¹²⁵I-labeled B16BL6-derived exosomes (approximately 2 μg exosomes; radiation dose, 37 kBq/mouse) were injected into tumor tissues of mice having tumor volume of 100–200 or 300–500 mm^3 . The mice were killed at an indicated time after the injection, and their blood was collected from the vena cava. Next, their organs were collected and were washed with saline. Radioactivity of each sample was measured using Wizard 1470 automatic gamma counter (PerkinElmer, Waltham, MA, USA). Results are expressed as %ID/ml for blood samples and as %ID/organ for other samples.

Microscopic observation of the cellular uptake of intratumorally injected exosomes in tumor tissues of mice. Tumor-bearing mice were intratumorally injected with PKH26-labeled exosomes at a dose of 10 μg exosome protein. The mice were sacrificed at an indicated time after the injection, and their tumor tissues were harvested and embedded in Tissue-Tek OCT compound (Sakura Finetek Japan, Tokyo, Japan). In addition, their organs were removed, were frozen at -80°C , and were sectioned into 10- μm -thick sections by using a freezing microtome (Leica CM3050 S; Leica Biosystems, Nussloch,

Germany). The sections were air dried and were fixed with 4% paraformaldehyde in PBS (Nacalai Tesque). Next, the sections were washed with PBS and were incubated with 0.1% polyoxyethylene (10) octylphenyl ether (Wako, Osaka, Japan) in PBS for 10 min at room temperature to induce permeabilization. The sections were then incubated with 20% FBS/PBS for 1 h at 37°C. After washing, the sections were treated with rabbit anti-Pmel17 antibody (dilution, 1:50; Santa Cruz Biotechnology) and rat anti-CD206 antibody (dilution, 1:200; AbD Serotec, Oxford, UK) for 1 h to stain B16BL6 cells and macrophages, respectively. Next, the sections were stained with Alexa Fluor 488-labeled goat anti-rabbit IgG (dilution, 1:250; Abcam) and Alexa Fluor 488-labeled goat anti-rat IgG (dilution, 1:200; Abcam) secondary antibodies. The sections were then treated with 100 nM DAPI for 5 min to stain the nuclei, were washed once with PBS, and were examined under the confocal laser-scanning microscope (AIR-MP).

Flow cytometric analysis of the cellular uptake of intratumorally injected exosomes in tumor tissues of mice. Tumor-bearing mice were intratumorally injected with PKH67-labeled exosomes at a dose of 20 μg exosome proteins. The mice were killed at an indicated time after the injection, and their tumor tissues were harvested. The tumor tissues were minced and were digested by incubating with type 4 collagenase (Worthington Biochemical Corp, Lakewood, NJ, USA) for 15 min at 37°C. Single-cell suspensions were prepared by filtering the tissue samples through a 40- μm strainer (Greiner Bio-One, Frickenhausen, Germany). The cell suspensions were fixed with 4% paraformaldehyde in PBS. After washing with PBS, the cell suspensions were incubated with 0.1% polyoxyethylene (10) octylphenyl ether for 10 min at room temperature to induce permeabilization. After washing, the cell suspensions were incubated with 5% FBS/PBS for 30 min at room temperature. Next, the cell suspensions were incubated with rabbit anti-Pmel17 antibody (dilution, 1:1000; Santa Cruz Biotechnology) for 1 h, followed by incubation with donkey anti-rabbit IgG H&L Alexa Fluor 647 (dilution, 1:2000; Abcam) secondary antibody. MFI of individual cells were evaluated using the Gallios Flow Cytometer, and data were analyzed using the Kaluza software.

Effect of B16BL6-derived exosomes on tumor growth. Tumor-bearing mice were intratumorally injected with PBS or 10 μg B16BL6-derived exosomes at 3-day intervals, and tumor size was measured every day.

Effect of GW4869 on tumor growth. Tumor-bearing mice were intratumorally injected with PBS, vehicle (5% DMSO), or 1 μg GW4869 at every day, and tumor size was measured every day.

Statistical analysis. Differences among groups were evaluated using Tukey-Kramer method, and $P < 0.05$ was considered statistically significant.

Results

B16BL6-derived exosomes approximately 100 nm in diameter. Figure 1(a) shows a TEM image of B16BL6-derived exosomes. Round-shaped vesicles of $\sim 100 \text{ nm}$ in diameter were observed. The particle size of B16BL6-derived exosomes measured by qNano was $97 \pm 3 \text{ nm}$ (Fig. 1b).

Cultured B16BL6 cells took up B16BL6-derived exosomes. Figure 1(c) shows the confocal microscopic images of B16BL6 cells incubated with PKH26-labeled, B16BL6-derived exosomes. Our results showed that PKH26-labeled exosomes were taken up by B16BL6 cells. In addition, results of flow

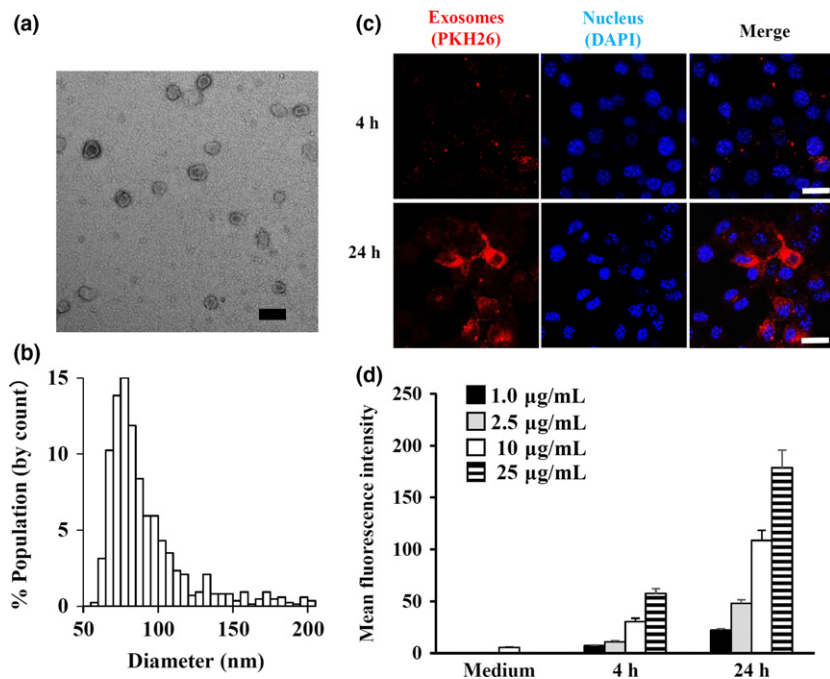


Fig. 1. *In vitro* uptake of fluorescently labeled B16BL6-derived exosomes. (a) Electron microscopic image of exosomes collected from B16BL6 cells. Scale bar = 100 nm. (b) Histogram of the particle size distribution of the B16BL6-derived exosomes determined using a qNano. (c) Confocal microscopic observation of B16BL6 cells incubated with PKH26-labeled exosomes (red) for 4 and 24 h; scale bar = 20 µm. (d) Flow cytometric analysis of B16BL6 cells incubated with the indicated concentrations of PKH67-labeled exosomes for 4 and 24 h. Results are expressed as mean + standard deviation of four wells.

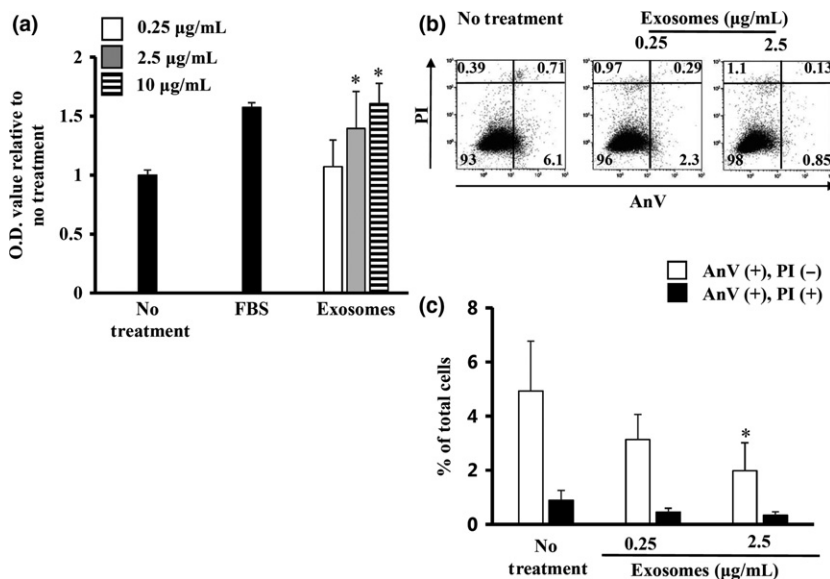


Fig. 2. Effect of B16BL6-derived exosomes on B16BL6 cell proliferation and apoptosis. (a) The number of B16BL6 cells treated with the indicated concentrations of B16BL6-derived exosomes was determined by performing the MTT assay. (b, c) After incubation with B16BL6-derived exosomes, B16BL6 cells were stained with AnV/PI and were analyzed by performing flow cytometry. (b) Representative flow cytometry plots of B16BL6 cells treated with or without B16BL6-derived exosomes. (c) Percentages of AnV-positive and PI-negative (AnV[+] and PI[-]) cells or AnV-positive and PI-positive (AnV[+] and PI[+]) cells were quantified. Results are expressed as mean + standard deviation of four wells; **P* < 0.05 compared with non-treatment cells.

cytometry analysis showed that the uptake of PKH67-labeled, B16BL6-derived exosomes by B16BL6 cells increased in a concentration- and time-dependent manner (Fig. 1d).

B16BL6-derived exosomes induced the proliferation and inhibited the apoptosis of B16BL6 cells. Next, we evaluated the effect of B16BL6-derived exosomes on the proliferation of cultured B16BL6 cells. Treatment with B16BL6-derived exosomes (2.5 and 10 µg/mL) significantly increased the number of B16BL6 cells compared with that of untreated cells (Fig. 2a). In particular, the number of B16BL6 cells treated with 10 µg/mL B16BL6-derived exosomes was comparable to that of cells cultured with 10% FBS. Next, we determined the antiapoptotic activity of B16BL6-derived exosomes by staining B16BL6 cells with AnV and PI (Fig. 2b). AnV-positive and PI-negative (AnV[+] and PI[-]) cells and AnV-positive and PI-positive (AnV[+] and PI[+]) cells were regarded as early apoptotic cells

and late apoptotic/necrotic cells, respectively.⁽¹⁴⁾ The percentage of AnV(+) and PI(-) cells was significantly lower among B16BL6 cells treated with 2.5 µg/mL B16BL6-derived exosomes than among untreated cells (Fig. 2c), suggesting that B16BL6-derived exosomes inhibited the apoptosis of B16BL6 cells. In addition, exosome treatment decreased the percentage of AnV(+) and PI(+) cells among B16BL6 cells; however, the decrease was not statistically significant.

B16BL6-derived exosomes regulated the levels of cell proliferation- and apoptosis-related proteins. Next, we investigated the effect of B16BL6-derived exosomes on the levels of intracellular proteins associated with cell proliferation (cyclin D1 and Akt) and apoptosis (Bcl-2, Bax; Fig. 3a). Cellular levels of cyclin D1, Bcl-2, and p-Akt increased, whereas those of Bax considerably decreased after treatment with B16BL6-derived exosomes. Western blotting detected survivin, an apoptotic

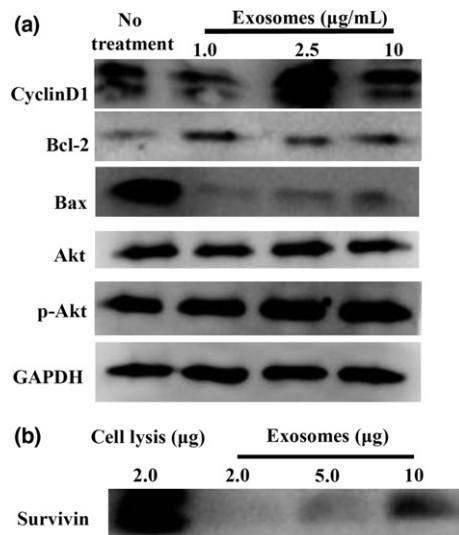


Fig. 3. Changes in the intracellular levels of cell proliferation- and apoptosis-related proteins after treatment with B16BL6-derived exosomes. (a) Western blotting analysis of cyclinD1, Bcl-2, Bax, Akt, p-Akt, and GAPDH expression in B16BL6 cells treated with the indicated concentrations of B16BL6-derived exosomes for 24 h. (b) Western blotting analysis of survivin expression in B16BL6 cells and B16BL6-derived exosomes.

inhibitor, in both B16BL6 cells and B16BL6-derived exosomes; however, its level in B16BL6-derived exosomes was lower than that in B16BL6 cells (Fig. 3b).

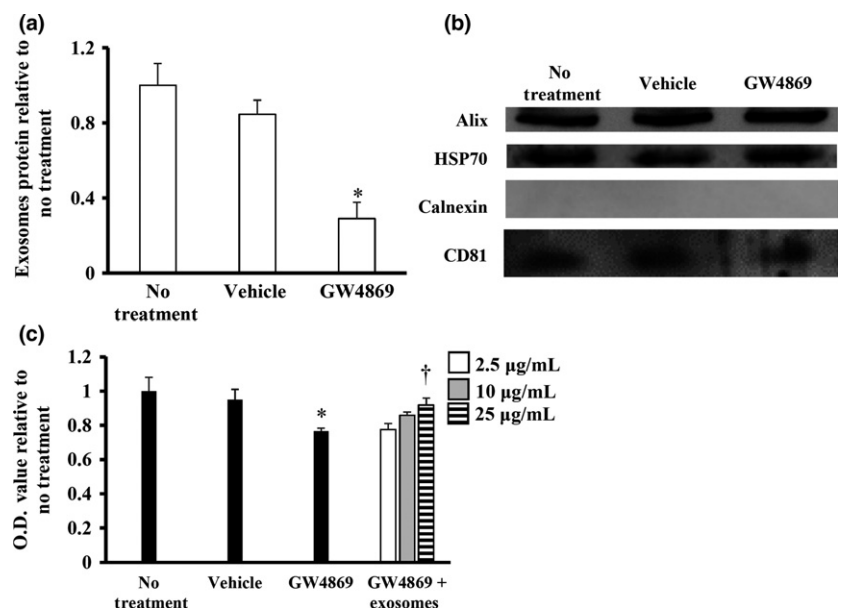
GW4869-induced inhibition of exosome secretion suppressed the proliferation of B16BL6 cells. Figure 4(a) shows protein levels in exosomes collected from B16BL6 cells treated with or without GW4869. GW4869 treatment significantly decreased the amount of collected exosomes to approximately 25% of that collected from untreated cells. Next, proteins present in exosomes collected from B16BL6 cells treated with or without GW4869 were analyzed by performing western blotting. Results of western blotting showed that exosome marker

proteins Alix, HSP70, and CD81 were present and that calnexin, an endoplasmic reticulum marker, was absent in all the three groups (exosomes derived from non-treatment, DMSO-treated, and GW4869-treated cells; Fig. 4b). GW4869 treatment significantly decreased the number of B16BL6 cells compared with that of untreated and vehicle-treated cells, implying that GW4869-induced inhibition of exosome secretion suppressed the proliferation of B16BL6 cells. In contrast, treatment of GW4869-treated B16BL6 cells with 25 µg/mL B16BL6-derived exosomes restored their proliferation rate (Fig. 4c).

Intratumorally injected B16BL6-derived exosomes remained in tumor tissue and accelerated its growth. Figure 5 shows the distribution of ^{125}I radioactivity after the injection of radiolabeled B16BL6-derived exosomes into tumors with a volume of 100–200 (Fig. 5a) or 300–500 mm³ (Fig. 5b). When radiolabeled B16BL6-derived exosomes were injected into tumors with low volume (Fig. 5a), a large fraction of the radioactivity remained within the tumors (approximately 57%, 43%, 33%, and 34% at 1, 4, 8, and 24 h after the injection, respectively), with limited distribution to other organs until 48 h after the injection. When radiolabeled B16BL6-derived exosomes were injected into tumors with large volume (300–500 mm³), a large fraction of the radioactivity remained within the tumors (Fig. 5b), which was similar to that observed for small tumors, with some radioactivity being detected in the lungs and liver (1.6% and 17% at 1 h, respectively).

B16BL6 cells efficiently took up intratumorally injected PKH26-labeled, B16BL6-derived exosomes. To determine cell types involved in the uptake of B16BL6-derived exosomes in tumor tissue, the mice were intratumorally injected with PKH26-labeled, B16BL6-derived exosomes and tumor sections obtained were stained with antibodies against gp100 (a melanoma marker) or CD206 (a macrophage marker). As shown in Figure 5(c,d), exosomes (red dots) colocalized with stained cells (green dots), indicating that PKH26-labeled, B16BL6-derived exosomes were taken up by both B16BL6 cells and macrophages present in the tumor tissue. However, the uptake efficiency between B16BL6 cells and macrophages seems to be different. PKH26-labeled, B16BL6-derived exosomes

Fig. 4. Effect of GW4869 on exosome secretion and B16BL6 cell number. (a) Exosomes were collected from B16BL6 cells treated with or without GW4869. The amount of collected exosomes was estimated by measuring protein concentration. (b) Western blotting of exosome marker proteins Alix, HSP70, and CD81 and exosome negative marker calnexin in exosomes isolated from B16BL6 cells treated with or without GW4869. (c) B16BL6 cells were treated with or without GW4869, and MTT assay was performed to estimate B16BL6 cell number. Moreover, B16BL6 cells were incubated with the indicated concentrations of GW4869 and B16BL6-derived exosomes, and cell number was estimated. * $P < 0.05$ compared with untreated and vehicle-treated cells; † $P < 0.05$ compared with GW4869-treated cells.



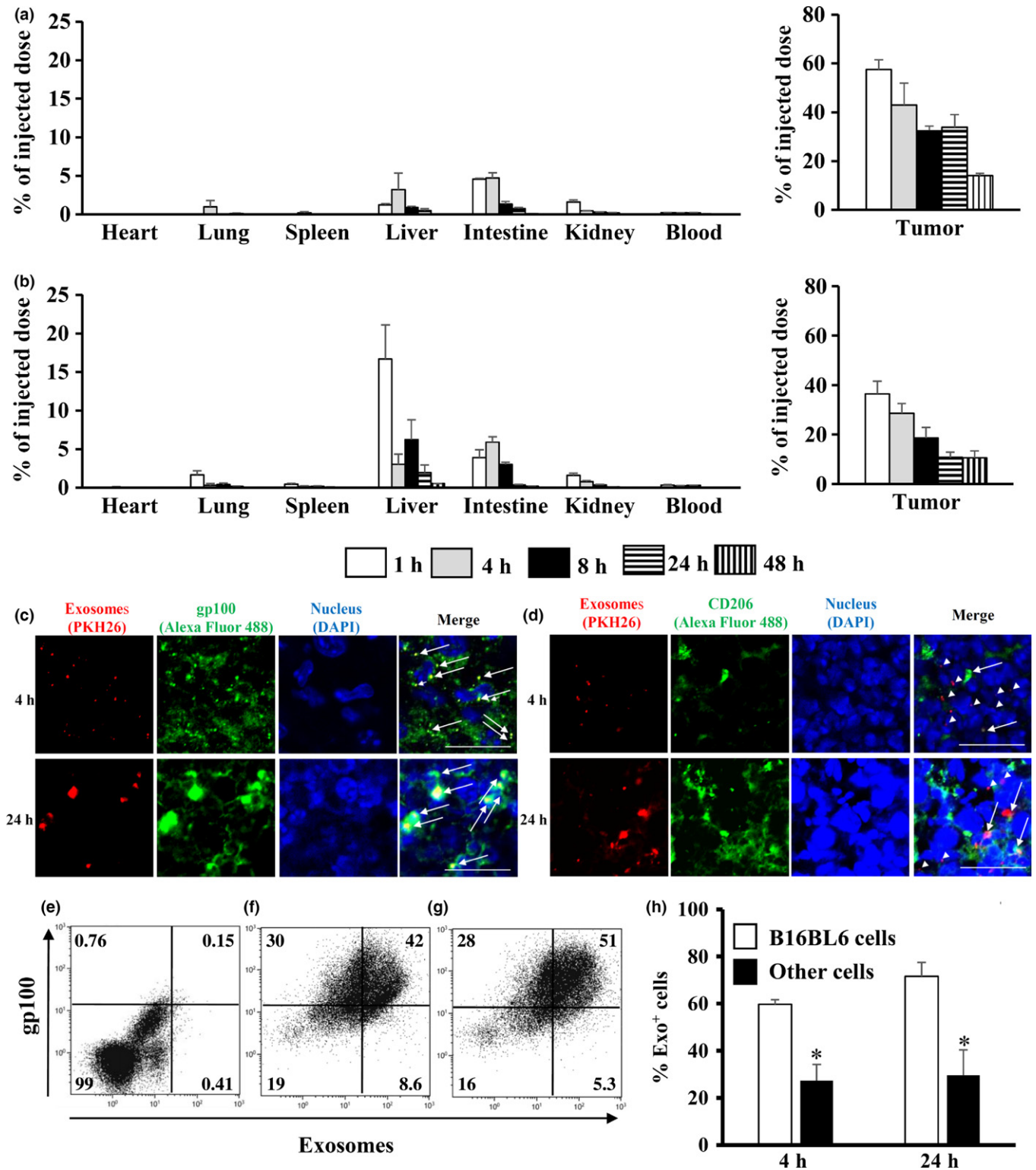


Fig. 5. Distribution and cellular uptake of intratumorally injected B16BL6-derived exosomes. (a, b) *In vivo* distribution of ¹²⁵I-labeled exosomes injected into tumor tissues with a volume of (a) 100–200 or (b) 300–500 mm³. Tumor tissues were collected at the indicated time after injection and were analyzed. Results are expressed as mean + standard error of mean of four mice. (c, d) After the intratumoral injection of PKH26-labeled, B16BL6-derived exosomes (red), tumor sections were prepared and were stained with antibodies against (c) gp100 (a melanoma marker; green) and (d) CD206 (a macrophage marker; green). The sections were examined under the confocal laser-scanning microscope. Arrowheads and arrows indicate single red dots and red dots merged with green dots, respectively; scale bar = 20 μm. (e–g) Flow cytometric analysis of the cellular uptake of intratumorally injected PKH67-labeled, B16BL6-derived exosomes in the tumor tissue. (e–g) Representative flow cytometry plots of B16BL6 and other cell populations after (f) 4 and (g) 24 h in mice injected with the exosomes (e; non-treatment group). Percentages of cells in each area of the plots were quantified and are shown in the plots. (h) Percentages of exosome-positive cells at 4 and 24 h after the intratumoral injection of PKH67-labeled exosomes. Results are expressed as mean + standard deviation of five mice; **P* < 0.05 compared with other cells.

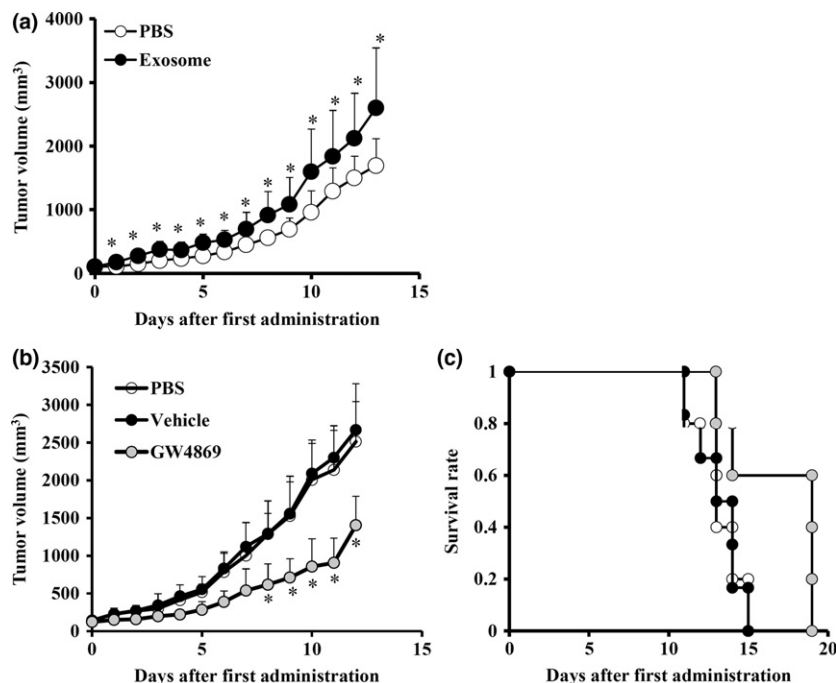


Fig. 6. Effect of B16BL6-derived exosomes and GW4869 on tumor progression. (a) Effect of exosomes on tumor growth. B16BL6-derived exosomes or PBS were intratumorally injected into tumor-bearing mice on days 0, 3, and 6. Tumor size was measured every day. Results are expressed as mean tumor volume (mm^3) + standard deviation of ten mice; * $P < 0.05$ compared with PBS-treated mice. (b, c) Effect of GW4869 on tumor growth and survival. Results are expressed as mean tumor volume (mm^3) + standard deviation of six mice; * $P < 0.05$ compared with PBS- and vehicle-treated mice.

colocalized more with B16BL6 cells than with macrophages (Fig. 5c,d). Next, we performed flow cytometric analysis to quantitatively investigate the uptake of PKH67-labeled exosomes by B16BL6 cells in tumor tissues (Fig. 5e,g). Results of flow cytometric analysis showed that approximately 60% and 70% B16BL6 cells took up PKH67-labeled, B16BL6-derived exosomes at 4 (Fig. 5f,h) and 24 h (Fig. 5g,h), respectively, and that approximately 27% and 30% other cells took up PKH67-labeled, B16BL6-derived exosomes at 4 (Fig. 5f,h) and 24 h (Fig. 5g,h), respectively.

Effects of B16BL6-derived exosomes and GW4869 on tumor growth. Figure 6(a) shows the time course of increase in tumor volume in tumor-bearing mice intratumorally injected with PBS or B16BL6-derived exosomes. Mice injected with B16BL6-derived exosomes showed significant increase in tumor growth compared with mice injected with PBS. Next, we investigated the effects of repeated intratumoral injections of GW4869 on tumor growth and survival in B16BL6-bearing mice (Fig. 6b,c). Intratumoral injection of GW4869 significantly reduced tumor growth. In addition, GW4869 treatment prolonged the survival of tumor-bearing mice compared with that of mice in other groups; however, the difference was not statistically significant.

Discussion

Cyclin D1 accelerates the G1 phase of the cell cycle to increase cell proliferation.⁽¹⁵⁾ Bcl-2 inhibits caspase-9 and caspase-3 activities and suppresses proapoptotic Bax proteins.^(16,17) PI3K/Akt signaling pathways play a role in the survival of different cell types.⁽¹⁸⁾ Therefore, B16BL6-derived exosome-induced increase in the proliferation of and inhibition of the apoptosis of B16BL6 cells may involve regulation of the intracellular levels of the above mentioned proteins (Figs 2,3a).

Survivin enhances cell proliferation and survival⁽¹⁹⁾ and activates cyclin-dependent kinase 4 (Cdk4) to generate a cyclinD1/Cdk4 complex.^(19,20) This complex promotes cell

cycle progression. Moreover, alternatively spliced survivin variants interact with Bcl-2 and inhibit caspase 3 activity in the mitochondria.⁽²¹⁾ It has been reported that survivin level in the exosomes derived from bladder cancer cells was higher than that in the lysate of the cancer cells and the exosomes enhanced the proliferation and survival of cancer cells.⁽²²⁾ Our results showed that B16BL6-derived exosomes also contained survivin; however, its level was lower than that in cell lysates (Fig. 3b). B16BL6-derived exosomes were efficiently taken up by B16BL6 cells (Fig. 1), suggesting that survivin present in the exosomes was delivered to B16BL6 cells and induced their proliferation and survival (Figs 2,3b).

GW4869 is a potent, cell-permeable, specific, and non-competitive inhibitor of neutral sphingomyelinases.⁽²³⁾ Exosome secretion is modulated by neutral sphingomyelinases and is inhibited by GW4869.^(24–26) We treated cells with GW4869 (5 $\mu\text{g}/\text{mL}$), which is considered to have no cytotoxic effect.⁽²⁴⁾ In the present study, the degree of the reduction in exosome secretion by GW4869 was much greater than the degree of the reduction in the cell number (Fig. 4a–c), indicating that the reduced exosome secretion by GW 4869 is not simply due to the reduced cell number. Moreover, reduction in the cell number by GW4869 was recovered by treating the cells with B16BL6-derived exosomes (Fig. 4c), suggesting that GW4869-induced suppression of B16BL6 cell proliferation was caused by the inhibition of exosome secretion.

Growth of tumor tissue increases vascular permeability in the tissue because of angiogenesis.^(27,28) A previous study showed that biodistribution of nanoparticles having sizes comparable to those of exosomes after intratumoral injection depended on tumor size.⁽²⁷⁾ Consistently, results of the present study showed that biodistribution of radiolabeled exosomes was different between mice with different sized tumors (Fig. 5a,b). In addition, distribution of some intratumorally injected radiolabeled exosomes to the liver and lungs suggested a leakage of exosomes into blood circulation because intravenously injected B16BL6-derived exosomes accumulate

in the liver or lungs.^(10,12) The recovery rate of radioactivity was approximately 60%. This might be because of the leakage of the radiolabeled exosomes from the tumor tissue to the surrounding skin or muscle.

Tumor tissues contain stromal cells as well as cancer cells, and cancer cell-derived exosomes may be taken up by both these cells. In the present study, we evaluated the uptake of B16BL6-derived exosomes by B16BL6 cells and macrophages, a type of stromal cells. Exosome uptake by macrophages was investigated because macrophages play a major role in the uptake of exogenously administered exosomes.⁽¹²⁾ Flow cytometric analysis and microscopic observation showed that B16BL6 cells efficiently took up B16BL6-derived exosomes compared with other cells in the tumor tissue (Fig. 6). This might be because exosomes are more efficiently taken up by cells similar to the producing cells than other cells,^(29,30) suggesting that B16BL6-derived exosomes have tropism toward B16BL6 cells. Research on uptake mechanism of cancer cell-derived exosomes by their producing cells is required in the future study.

Cancer cell-derived exosomes induce tumor progression both *in vitro* and *in vivo*.^(29–33) Significant increase in tumor volume after the intratumoral injection of B16BL6-derived exosomes (Fig. 6a) suggests that these exosomes induced tumor progression. In contrast, intratumoral injection of GW4869 inhibited tumor progression (Fig. 6b,c). Because B16BL6-derived exosomes remain in the tumor tissue and are mainly taken up by B16BL6 cells (Fig. 5), it can be suggested that these exosomes promote B16BL6 cell proliferation and tumor progression under physiological conditions.

In conclusion, we found that B16BL6 cells secreted and took up their own exosomes to induce their proliferation and inhibit their apoptosis, thus promoting tumor progression. These findings provide important information for elucidating the physiological functions of exosomes.

Disclosure Statement

All authors have no conflict of interest.

References

- Bakhshandeh B, Kamaledin MA, Aalishah K. A comprehensive review on exosomes and microvesicles as epigenetic factors. *Curr Stem Cell Res Ther* 2016; **12**: 31–36.
- Suchorska WM, Lach MS. The role of exosomes in tumor progression and metastasis (review). *Oncol Rep* 2016; **35**: 1237–44.
- Costa-Silva B, Aiello NM, Ocean AJ *et al*. Pancreatic cancer exosomes initiate pre-metastatic niche formation in the liver. *Nat Cell Biol* 2015; **17**: 816–26.
- Peinado H, Aleckovic M, Lavotshkin S *et al*. Melanoma exosomes educate bone marrow progenitor cells toward a pro-metastatic phenotype through MET. *Nat Med* 2012; **18**: 883–91.
- Valadi H, Ekstrom K, Bossios A, Sjostrand M, Lee JJ, Lotvall JO. Exosome-mediated transfer of mRNAs and microRNAs is a novel mechanism of genetic exchange between cells. *Nat Cell Biol* 2007; **9**: 654–9.
- Hoshino A, Costa-Silva B, Shen TL *et al*. Tumour exosome integrins determine organotropic metastasis. *Nature* 2015; **527**: 329–35.
- Tominaga N, Kosaka N, Ono M *et al*. Brain metastatic cancer cells release microRNA-181c-containing extracellular vesicles capable of destructing blood-brain barrier. *Nat Commun* 2015; **6**: 6716.
- Ge R, Tan E, Sharghi-Namini S, Asada HH. Exosomes in cancer microenvironment and beyond: have we overlooked these extracellular messengers? *Cancer Microenviron* 2012; **5**: 323–32.
- Kahlert C, Kalluri R. Exosomes in tumor microenvironment influence cancer progression and metastasis. *J Mol Med (Berl)* 2013; **91**: 431–7.
- Morishita M, Takahashi Y, Nishikawa M *et al*. Quantitative analysis of tissue distribution of the B16BL6-derived exosomes using a streptavidin-lactadherin fusion protein and iodine-125-labeled biotin derivative after intravenous injection in mice. *J Pharm Sci* 2015; **104**: 705–13.
- Takahashi Y, Nishikawa M, Shinotsuka H *et al*. Visualization and *in vivo* tracking of the exosomes of murine melanoma B16-BL6 cells in mice after intravenous injection. *J Biotechnol* 2013; **165**: 77–84.
- Imai T, Takahashi Y, Nishikawa M *et al*. Macrophage-dependent clearance of systemically administered B16BL6-derived exosomes from the blood circulation in mice. *J Extracell Vesicles* 2015; **4**: 26238.
- Yamashita T, Takahashi Y, Nishikawa M, Takakura Y. Effect of exosome isolation methods on physicochemical properties of exosomes and clearance of exosomes from the blood circulation. *Eur J Pharm Biopharm* 2016; **98**: 1–8.
- Wlodkowic D, Skommer J, Darzynkiewicz Z. Flow cytometry-based apoptosis detection. *Methods Mol Biol* 2009; **559**: 19–32.
- Baldin V, Lukas J, Marcote MJ, Pagano M, Draetta G. Cyclin D1 is a nuclear protein required for cell cycle progression in G1. *Genes Dev* 1993; **7**: 812–21.
- Cory S, Huang DC, Adams JM. The bcl-2 family: roles in cell survival and oncogenesis. *Oncogene* 2003; **22**: 8590–607.
- Swanton E, Savory P, Cosulich S, Clarke P, Woodman P. Bcl-2 regulates a caspase-3/caspase-2 apoptotic cascade in cytosolic extracts. *Oncogene* 1999; **18**: 1781–7.
- Hennessy BT, Smith DL, Ram PT, Lu Y, Mills GB. Exploiting the PI3K/AKT pathway for cancer drug discovery. *Nat Rev Drug Discov* 2005; **4**: 988–1004.
- Altieri DC. Survivin, cancer networks and pathway-directed drug discovery. *Nat Rev Cancer* 2008; **8**: 61–70.
- Ito T, Shiraki K, Sugimoto K *et al*. Survivin promotes cell proliferation in human hepatocellular carcinoma. *Hepatology* 2000; **31**: 1080–5.
- Wang HW, Sharp TV, Koumi A, Koentges G, Boshoff C. Characterization of an anti-apoptotic glycoprotein encoded by kaposi's sarcoma-associated herpesvirus which resembles a spliced variant of human survivin. *EMBO J* 2002; **21**: 2602–15.
- Yang L, Wu XH, Wang D, Luo CL, Chen LX. Bladder cancer cell-derived exosomes inhibit tumor cell apoptosis and induce cell proliferation *in vitro*. *Mol Med Rep* 2013; **8**: 1272–8.
- Luberto C, Hassler DF, Signorelli P *et al*. Inhibition of tumor necrosis factor-induced cell death in MCF7 by a novel inhibitor of neutral sphingomyelinase. *J Biol Chem* 2002; **277**: 41128–39.
- Essandoh K, Yang L, Wang X *et al*. Blockade of exosome generation with GW4869 dampens the sepsis-induced inflammation and cardiac dysfunction. *Biochim Biophys Acta* 2015; **1852**: 2362–71.
- Guo BB, Bellingham SA, Hill AF. The neutral sphingomyelinase pathway regulates packaging of the prion protein into exosomes. *J Biol Chem* 2015; **290**: 3455–67.
- Li J, Liu K, Liu Y *et al*. Exosomes mediate the cell-to-cell transmission of IFN-alpha-induced antiviral activity. *Nat Immunol* 2013; **14**: 793–803.
- Rohner NA, Thomas SN. Melanoma growth effects on molecular clearance from tumors and biodistribution into systemic tissues versus draining lymph nodes. *J Control Release* 2016; **223**: 99–108.
- Weis SM, Cheresch DA. Tumor angiogenesis: molecular pathways and therapeutic targets. *Nat Med* 2011; **17**: 1359–70.
- Hazan-Halevy I, Rosenblum D, Weinstein S, Bairey O, Raanani P, Peer D. Cell-specific uptake of mantle cell lymphoma-derived exosomes by malignant and non-malignant B-lymphocytes. *Cancer Lett* 2015; **364**: 59–69.
- Rana S, Yue S, Stadel D, Zoller M. Toward tailored exosomes: the exosomal tetraspanin web contributes to target cell selection. *Int J Biochem Cell Biol* 2012; **44**: 1574–84.
- Raimondo S, Saieva L, Corrado C *et al*. Chronic myeloid leukemia-derived exosomes promote tumor growth through an autocrine mechanism. *Cell Commun Signal* 2015; **13**: 8.
- Sento S, Sasabe E, Yamamoto T. Application of a persistent heparin treatment inhibits the malignant potential of oral squamous carcinoma cells induced by tumor cell-derived exosomes. *PLoS One* 2016; **11**: e0148454.
- Qu JL, Qu XJ, Zhao MF *et al*. Gastric cancer exosomes promote tumour cell proliferation through PI3K/Akt and MAPK/ERK activation. *Dig Liver Dis* 2009; **41**: 875–80.